

Indications of a spatial variation of the fine structure constant

J. K. Webb¹, J. A. King¹, M. T. Murphy², V. V. Flambaum¹, R. F. Carswell³, and M. B. Bainbridge¹

¹*School of Physics, University of New South Wales, Sydney, NSW 2052, Australia*

²*Centre for Astrophysics and Supercomputing, Swinburne University of Technology,
Mail H30, PO Box 218, Victoria 3122, Australia and*

³*Institute of Astronomy, Madingley Road, Cambridge, CB3 0HA, England.*

(Dated: November 2, 2011)

We previously reported Keck telescope observations suggesting a smaller value of the fine structure constant, α , at high redshift. New Very Large Telescope (VLT) data, probing a different direction in the universe, shows an inverse evolution; α increases at high redshift. Although the pattern could be due to as yet undetected systematic effects, with the systematics as presently understood the combined dataset fits a spatial dipole, significant at the 4.2σ level, in the direction right ascension 17.5 ± 0.9 hours, declination -58 ± 9 degrees. The independent VLT and Keck samples give consistent dipole directions and amplitudes, as do high and low redshift samples. A search for systematics, using observations duplicated at both telescopes, reveals none so far which emulate this result.

PACS numbers: 06.20.Jr, 95.30.Dr, 95.30.Sf, 98.62.Ra, 98.80.-k, 98.80.Es, 98.80.Jk

Quasar spectroscopy as a test of fundamental physics.— The vast light-travel times to distant quasars allow us to probe physics at high redshift. The relative wavenumbers, ω_z , of atomic transitions detected at redshift $z = \lambda_{obs}/\lambda_{lab} - 1$, can be compared with laboratory values, ω_0 , via the relationship $\omega_z = \omega_0 + Q(\alpha_z^2 - \alpha_0^2)/\alpha_0^2$ where the coefficient Q measures the sensitivity of a given transition to a change in α . The variation in both magnitude and sign of Q for different transitions is a significant advantage of the Many Multiplet method [1, 2], helping to combat potential systematics.

The first application of this method, 30 measurements of $\Delta\alpha/\alpha = (\alpha_z - \alpha_0)/\alpha_0$, indicated a smaller α at high redshift at the 3σ significance level. By 2004 we had made 143 measurements of α covering a wide redshift range, using further data from the Keck telescope obtained by 3 separate groups, supporting our earlier findings, that towards that general direction in the universe at least, α may have been smaller at high redshift, at the 5σ level [3–5]. The constant factor at that point was (undesirably) the telescope and spectrograph.

New data from the VLT.— We have now analysed a large dataset from a different observatory, the VLT. Full details and searches for systematic errors will be given elsewhere [6, 7]. Here we summarize the evidence for spatial variation in α emerging from the combined Keck+VLT samples. Quasar spectra, obtained from the ESO Science Archive, were selected, prioritising primarily by expected signal to noise but with some preference given to higher redshift objects and to objects giving more extensive sky coverage. The ESO MIDAS pipeline was used for the first data reduction step, including wavelength calibration, although enhancements were made to derive a more robust and accurate wavelength solution from an improved selection of thorium-argon calibration lamp emission lines [8]. Echelle spectral orders from several exposures of a given quasar were combined using UVES_POPLER [9]. A total of 60 quasar spectra from the

VLT have been used for the present work, yielding 153 absorption systems. Absorption systems were identified via a careful visual search of each spectrum, using RDGEN [10], scanning for commonly detected transitions at the same redshift, hence aligned in velocity coordinates. Several transition matches were required for acceptance and, given the high spectral resolution, chance matches were eliminated.

Absorption system modelling.— As in our previous studies, VPFIT was used to model the profiles in each absorption system [11] with some enhancements, described in [6]. A comprehensive list of the transitions used, their laboratory wavelengths, oscillator strengths, and Q coefficients are compiled in [4, 6].

The following general procedures were adhered to: (i) For each absorption system, physically related parameters (redshifts and b -parameters) are tied, in order to minimise the required number of free parameters and derive the strongest possible constraints on line positions, and hence $\Delta\alpha/\alpha$. (ii) Parameters were tied only for species with similar ionisation potentials, to minimise possible introduction of random effects on α , mimicked by spatial (and hence velocity) segregation effects; (iii) Line broadening is typically dominated by turbulent rather than thermal motion. Both limiting-case models were applied and $\Delta\alpha/\alpha$ determined for each. The final $\Delta\alpha/\alpha$ was derived from a likelihood-weighted average; (iv) Where appropriate and available, isotopic shifts and hyperfine structure are included in the fitting procedure; (v) Velocity structures were determined initially choosing the strongest unsaturated transitions in each system. Normalised residuals across each transition fitted were examined and the fit progressively refined with the introduction of each additional transition to the fit; (vi) Transitions falling in spectral regions contaminated by telluric features or atmospheric absorption were discarded. Any data regions contaminated by cosmic rays, faulty CCD pixels, or any other unidentified noise effects, were also

discarded; (vii) A few gravitational lenses were identified by being difficult or impossible to model successfully. The non-point source quasar image and the resultant complex line-of-sight geometry can significantly alter apparent relative line strengths. These systems were discarded; (viii) In all cases we derived the final model without solving for $\Delta\alpha/\alpha$. The introduction of $\Delta\alpha/\alpha$ as an additional free parameter was only done once the profile velocity structure had been finalised, eliminating any possible bias towards a ‘preferred’ $\Delta\alpha/\alpha$. One potential consequence of this approach might conceivably be a small bias on $\Delta\alpha/\alpha$ towards zero, should some ‘fitting-away’ of $\Delta\alpha/\alpha$ occur by column density adjustments or velocity structure decisions. The reverse is not true, i.e. it cannot bias towards a non-zero $\Delta\alpha/\alpha$. For details of all the points above see [6].

VPFIT [11] minimises χ^2 simultaneously over all species. Whilst the strongest components may appear in all species, weaker components can sometimes fall below the detection threshold and hence are excluded, such that a component which appears in MgII, for example, does not appear in FeII. There is no solution to this (known) problem but its effect merely adds an additional random scatter on $\Delta\alpha/\alpha$ for an ensemble of observations.

Spatially dependent α .— An initial inspection of $\Delta\alpha/\alpha$ vs redshift for the new VLT dataset reveals a redshift trend, opposite in sign compared to the earlier Keck data. Splitting each sample at $z = 1.8$, our 2004 Keck sample [5] gave $\langle\Delta\alpha/\alpha\rangle_{z<1.8} = -0.54 \pm 0.12 \times 10^{-5}$ and $\langle\Delta\alpha/\alpha\rangle_{z>1.8} = -0.74 \pm 0.17 \times 10^{-5}$. The present VLT sample, discussed in detail in [6], gives $\langle\Delta\alpha/\alpha\rangle_{z<1.8} = -0.06 \pm 0.16 \times 10^{-5}$ and $\langle\Delta\alpha/\alpha\rangle_{z>1.8} = +0.61 \pm 0.20 \times 10^{-5}$. Errors here and throughout this paper are 1σ estimates. Our VLT result above for $z < 1.8$ agrees with the VLT data presented in [12].

Errors on individual $\Delta\alpha/\alpha$ values for our VLT sample are $\sigma_{tot}^2 = \sigma_{stat}^2 + \sigma_{rand}^2$, where σ_{rand}^2 was derived empirically by fitting a constant $\Delta\alpha/\alpha$ to the sample, i.e. monopole-only, using a modification of the Least Trimmed Squares (LTS) method, where only 85% of data, those points with the smallest squared residuals, are fitted. σ_{rand} was assumed constant for all absorbers and found to be $\approx 0.9 \times 10^{-5}$, showing that the scatter in the VLT $\Delta\alpha/\alpha$ is greater than expected on the basis of statistical-errors alone. Errors on $\Delta\alpha/\alpha$ for the Keck sample are discussed in [4], although we derive a new estimate of $\sigma_{rand} = 1.74$ for the Keck points using the LTS method, again relative to a monopole-only fit to the Keck sample.

The Keck (Mauna Kea, Hawaii) and VLT (Paranal, Chile) locations on Earth are separated by 45° in latitude and hence, on average, observe different directions on the sky. The $\langle\Delta\alpha/\alpha\rangle$ results above suggest exploring a simple spatial dependence using the combined dataset.

The Keck sample we use is as presented in [5] with minor modifications: 3 points were removed. 2 had been

included erroneously (from a spectrum known to have calibration problems) and 1 further point was clipped, having a residual greater than 3σ against a modified LTS fit to the Keck data.

We fit 3 different models to the 3 datasets (i.e. Keck, VLT and combined samples). Initially we try a dipole+monopole model, $\Delta\alpha/\alpha = A \cos \Theta + m$, where m allows an offset from the terrestrial value, Θ is the angle on the sky between quasar sightline and best-fit dipole position, and A is the dipole amplitude. Noting the theoretical interpretation of the monopole term is unclear, we fit a second model, without the monopole, $\Delta\alpha/\alpha = A \cos \Theta$. Thirdly, in order to explore a possible spatial gradient in α , we assign a distance to each $\Delta\alpha/\alpha$ measurement of $r(z) = ct(z)$ where c is the speed of light and $t(z)$ is the look-back time at redshift z . The model is then $\Delta\alpha/\alpha = Ar \cos \Theta$.

To estimate the dipole significance we bootstrap the sample, repeatedly randomising the association between $\Delta\alpha/\alpha$ and the absorption system location in space (i.e. quasar sightline and absorption redshift). A dipole is fitted and its χ^2 derived at each realisation, to obtain a χ^2 probability distribution. This gives the probability of fitting a dipole to the data and obtaining a value of χ^2 less than or equal to that observed for the real sample by chance alone, i.e. the statistical significance of a dipole model compared to a monopole, and hence an uncertainty estimate for the dipole amplitude, A .

All 3 models give a detection significance in the range $4.1 - 4.2\sigma$ and the best-fit parameters and associated errors (given in the figure captions) vary only slightly. Figure 1 illustrates an all-sky map for the best-fit non-monopole model, using equatorial co-ordinates. Approximate 1σ error contours are derived from the covariance matrix. Figure 2 illustrates the $\Delta\alpha/\alpha$ binned data and the best-fit dipole+monopole model. Figure 3 illustrates $\Delta\alpha/\alpha$ vs look-back time distance projected onto the dipole axis, $r \cos \Theta$, using the best-fit dipole parameters for this model. This model seems to represent the data reasonably well and $\Delta\alpha/\alpha$ appears distance-dependent, the correlation being significant at the 4.2σ level.

An alternative to the LTS method described above, to allow for any unknown additional contribution to the errors on individual $\Delta\alpha/\alpha$ measurements, one can assume $\sigma_{tot}^2 = \sigma_{stat}^2$ and iteratively trim the sample during model fitting. This provides a further test of whether the apparent spatial gradient in α is dominated by a subset of the data, perhaps more prone to some unknown systematic than the remainder. Adopting $\sigma_{tot}^2 = \sigma_{stat}^2$ will tend to result in higher significance levels. Figure 4 illustrates this test and shows that the apparent dipole seems robust to data trimming.

Empirical test for systematics.— One potential systematic in the data could arise if there were slight mechanical mis-alignments of the slits for the 2 arms of the UVES spectrograph on the VLT. This could cause wave-

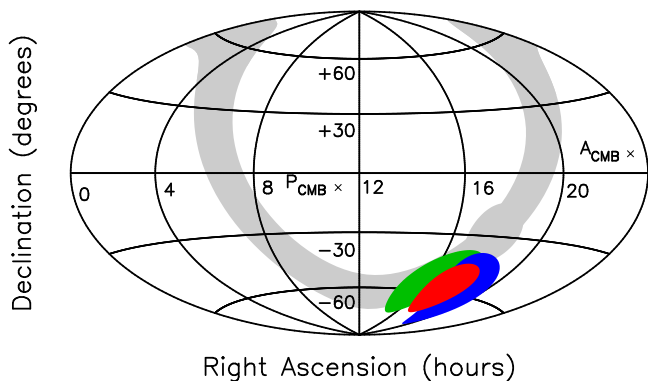


FIG. 1. All-sky plot in equatorial coordinates showing the independent Keck (green, leftmost) and VLT (blue, rightmost) best-fit dipoles, and the combined sample (red, centre), for the dipole model, $\Delta\alpha/\alpha = A \cos \Theta$, with $A = (1.02 \pm 0.21) \times 10^{-5}$. Approximate 1σ confidence contours are from the covariance matrix. The best-fit dipole is at right ascension 17.4 ± 0.9 hours, declination -58 ± 9 degrees and is statistically preferred over a monopole-only model at the 4.1σ level. For this model, a bootstrap analysis shows the chance-probability of the dipole alignments being as good or closer than observed is 6%. For a dipole+monopole model this increases to 14%. The cosmic microwave background dipole and antipole are illustrated for comparison.

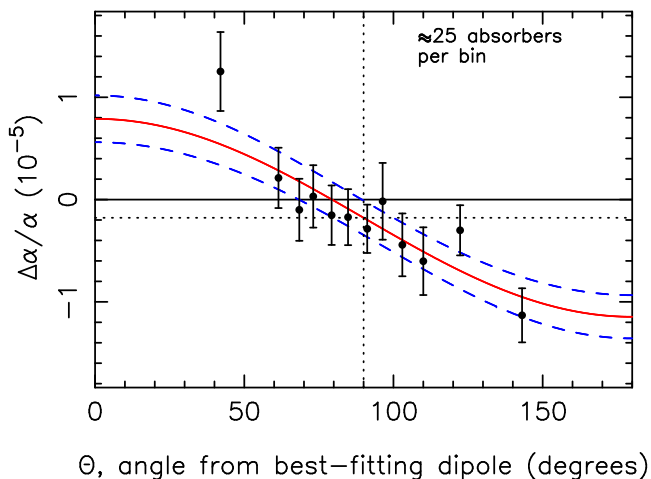


FIG. 2. $\Delta\alpha/\alpha$ for the combined Keck and VLT data vs angle Θ from the best-fit dipole position (best-fit parameters given in Figure 1 caption). Dashed lines illustrate $\pm 1\sigma$ errors. For a discussion on the monopole term, see [6].

length shifts between spectral features falling in the blue and red arms. However, this specific effect appears to be substantially smaller than required to explain values of $\Delta\alpha/\alpha \sim 10^{-5}$ seen in the present work [13].

A more subtle but related effect may be slight off-centre placement of the quasar image in the spectrograph slit, by different amounts for different exposures, at different wavelength settings. This may apply to either or both Keck and VLT spectra. Since spectrograph slit il-

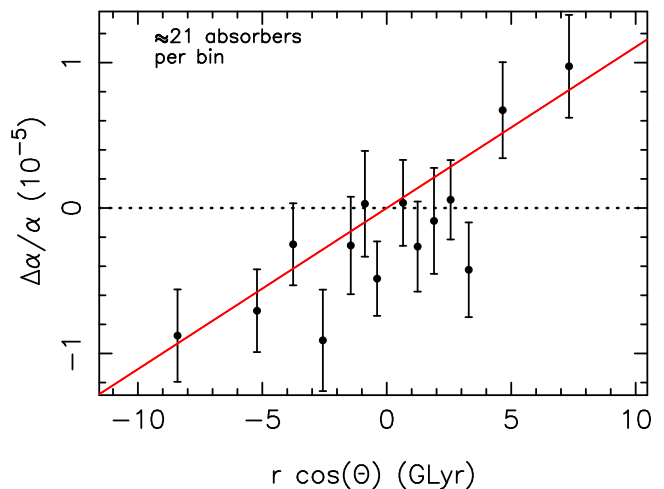


FIG. 3. $\Delta\alpha/\alpha$ vs $Ar \cos \Theta$ showing an apparent gradient in α along the best-fit dipole. The best-fit direction is at right ascension 17.5 ± 0.9 hours, declination -58 ± 9 degrees, for which $A = (1.1 \pm 0.25) \times 10^{-6} \text{ GLyr}^{-1}$. A spatial gradient is statistically preferred over a monopole-only model at the 4.2σ level. A cosmology with parameters $(H_0, \Omega_M, \Omega_\Lambda) = (70.5, 0.2736, 0.726)$ was used [18].

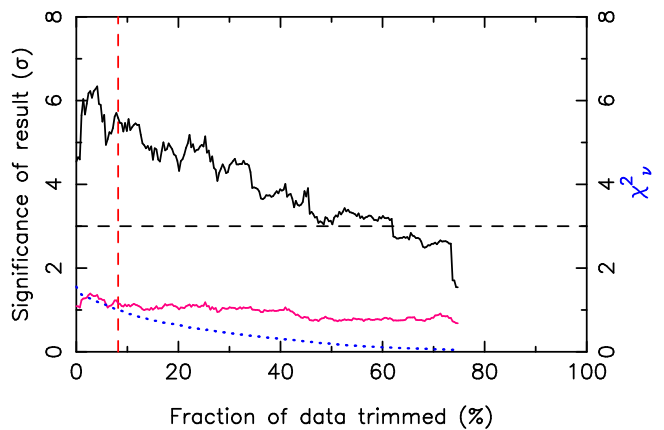


FIG. 4. As an alternative to increasing $\Delta\alpha/\alpha$ error bars, to account for the additional scatter in the data as described in the text, we instead use $\sigma_{tot}^2 = \sigma_{stat}^2$ and iteratively clip the most deviant $\Delta\alpha/\alpha$ value, fitting $\Delta\alpha/\alpha = Ar \cos \Theta$. Approximately 60% of the data must be discarded before the significance drops below 3σ showing the dipole signal is not due to a small subset of the data. The solid (pink) line at the bottom of the graph shows the dipole amplitude in units of $10^{-6} \text{ GLyr}^{-1}$. The dotted (blue) line at the bottom of the graph shows χ^2_ν and the vertical dashed (red) line illustrates $\chi^2_\nu = 1$ when $\sim 8\%$ of the data has been trimmed, at which point the significance is $\sim 5.5\sigma$

uminations are different for quasar (point source) and ThAr calibration lamp (uniform illumination), the subsequent combination of individual exposures to form a 1-dimensional spectrum may then contain relative velocity shifts between spectral segments coming from different exposures. This effect will exist in our data at some

level and it is clearly important to know the impact on an ensemble of measurements of α .

Fortunately, 6 quasars in our sample have both Keck and VLT spectra, allowing a direct and empirical check on the effect above, and indeed any other systematics which produce relative velocity shifts along the spectrum. To do this we selected small spectral segments, each a few Å wide, flanked by unabsorbed continuum flux from the quasar, and fitted Voigt profiles using VPFIT, but adding an additional free parameter allowing a velocity shift between the Keck and VLT segments, $\delta v(\lambda_{obs})_i$, where λ_{obs} is the observed wavelength and i refers to the i^{th} quasar. All available absorption lines in the 6 spectra were used, including both Lyman- α forest lines and heavy element lines but excluding telluric features. In this way we can map any effective relative distortions in the calibrations between each pair of spectra. A total of 694 measurements were used from the 6 pairs of spectra over the observed wavelength range $3506 < \lambda < 8945\text{Å}$.

We formed a composite function $\delta v(\lambda_{obs})$ after first normalising $\langle \delta v(\lambda_{obs})_i \rangle = 0$ for each i to remove any potential small constant velocity offsets from each spectrum (expected from off-centering of the quasar in the spectrograph slit), which cannot influence α .

Finally, we fit the composite $\delta v(\lambda_{obs})$ with a linear function $f(\delta v) = a\lambda_{obs} + b$ where $a = (-7 \pm 14) \times 10^{-5} \text{ km s}^{-1} \text{Å}^{-1}$, $b = 0.38 \pm 0.71 \text{ km s}^{-1}$. The final $f(\delta v)$ thus shows a weak (but statistically insignificant) velocity drift, and provides an empirical transformation between the Keck and VLT wavelength scales. For each VLT quasar absorption system, we modify the input laboratory wavelengths used in the Voigt profile fitting procedure λ_{lab} to $\lambda'_{lab} = \lambda_{lab} + \Delta\lambda_{lab}$ where $\Delta\lambda_{lab} = \lambda_{lab} \delta v(\lambda_{obs})/c$, and finally use the λ'_{lab} to re-compute $\Delta\alpha/\alpha$ for the entire sample.

There was one complicating aspect of this effect excluded from the discussion above, arising from a 7^{th} spectral pair. The $\delta v(\lambda_{obs})_7$ showed a more significant non-zero slope than the other 6, suggesting a small but significant calibration problem with that particular spectrum. We therefore applied a slightly more complicated transformation to the data to allow for this, using a Monte Carlo simulation to estimate the potential impact on our full combined Keck and VLT sample of both the previous effect measured in 6 quasars *plus* the effect derived from the 7^{th} quasar simultaneously, applied in appropriate proportions. The full details of this analysis will be discussed separately in [7].

A systematic of the same magnitude as that from the 7^{th} pair cannot be present in any large fraction of our data, otherwise it would generate large numbers of noticeable outliers. If we apply $f(\delta v)$ from the 6 quasar pairs, the significance of the dipole+monopole model $\Delta\alpha/\alpha = A\cos\Theta + m$, is reduced to 3.1σ . Blindly including the effect of the 7^{th} pair under a Monte Carlo method reduces the significance to a most likely value of

2.2σ . However, in this circumstance we introduce significant extra scatter into the data above that already observed, implying that it over-estimates any systematic effect of this type. Additionally, the trend of $\delta v(\lambda_{obs})_i$ against wavelength is different in magnitude and sign for each quasar pair, implying that these effects are likely to average out for an ensemble of observations. Thus, application of the effect as described above should be regarded as extreme in terms of impact on estimating $\Delta\alpha/\alpha$.

Conclusions.— Quasar spectra obtained using 2 separate observatories show a spatial variation in the relative spacings of absorption lines which could be due to an as yet undetected systematic effect, or a dipole variation of α . A fit to the dipole gives a significance of $\gtrsim 4.2\sigma$, assuming the error bars described above. Assuming a dipole interpretation, the two datasets exhibit internal consistency and the directions of the independently derived spatial dipoles agree. The magnitudes of the apparent $\Delta\alpha/\alpha$ variation in both datasets also agree. A subset of the quasar spectra observed at both observatories permits a direct test for systematics. So far, none are found which are likely to emulate the apparent cosmological dipole in α we detect. Consistency with other astronomical data is discussed in [14]. Consistency with laboratory, meteorite, and Oklo natural reactor is discussed in [15]. Short-wavelength oscillatory variations in the wavelength scale such as those reported by [16], [17], do not significantly impact on our results. To explain our results in terms of systematics would require at least 2 different, finely tuned, effects. Future similar measurements targeting the apparent pole and anti-pole directions will maximise detection sensitivity, and further observations duplicated on 2 independent telescopes will better constrain systematics. Most importantly, an independent technique is required to check these results. Qualitatively, our results could violate the equivalence principle and infer a very large or infinite universe, within which our ‘local’ Hubble volume represents a tiny fraction, with correspondingly small variations in the physical constants.

This work is supported by the Australian Research Council. We thank Steve Curran, Elliott Koch and Julian Berengut for discussions throughout this work.

-
- [1] J. K. Webb *et al.*, Phys. Rev. Lett. **82**, 884 (1999).
 - [2] V. A. Dzuba, V. V. Flambaum, and J. K. Webb, Phys. Rev. Lett. **82**, 888 (1999).
 - [3] J. K. Webb *et al.*, Phys. Rev. Lett. **87**, 091301 (2001).
 - [4] M. T. Murphy, J. K. Webb, and V. V. Flambaum, Mon. Not. Roy. Astron. Soc. **345**, 609 (2003).
 - [5] M. T. Murphy, V. V. Flambaum, and J. K. Webb, in *Astrophysics, Clocks and Fundamental Constants*, Lecture Notes in Physics (Springer, Berlin, Heidelberg, New York, 2004), Vol. 648, p. 131–150.

- [6] J. A. King *et al.*, “Spatial variation in the fine-structure constant – new results from VLT/UVES,” to be published.
- [7] F. E. Koch *et al.*, “Spatial variation in the fine-structure constant – a search for systematic effects,” to be published.
- [8] M. T. Murphy *et al.*, *Mon. Not. Roy. Astron. Soc.* **378**, 221 (2007).
- [9] M. T. Murphy, “UVES_POPLER,” (2010), http://astronomy.swin.edu.au/~mmurphy/UVES_popler.
- [10] R. F. Carswell, “RDGEN,” (2004), <http://www.ast.cam.ac.uk/~rfc/rdgen.html>.
- [11] R. F. Carswell and J. K. Webb, “VPFIT - Voigt profile fitting program. Version 9.5,” (2010), <http://www.ast.cam.ac.uk/~rfc/vpfit.html>.
- [12] R. Srianand, H. Chand, P. Petitjean, and B. Aracil, *Phys. Rev. Lett.* **99**, 239002 (2007).
- [13] P. Molaro *et al.*, *Astron. Astrophys.* **481**, 559 (2008).
- [14] J. C. Berengut, V. V. Flambaum, J. A. King, S. J. Curran, and J. K. Webb, *Phys. Rev. D* **83**, 123506 (2011).
- [15] J. C. Berengut and V. V. Flambaum, arXiv:1008.3957.
- [16] K. Griest, J. B. Whitmore, A. M. Wolfe, J. X. Prochaska, J. C. Howk, and G. W. Marcy, *Astrophys. J.* **708**, 158 (2010).
- [17] J. B. Whitmore, M. T. Murphy, and K. Griest, *Astrophys. J.* **723**, 89 (2010),.
- [18] G. Hinshaw *et al.*, *Astrophys. J. Supp. Ser.* **180**, 225 (2009).

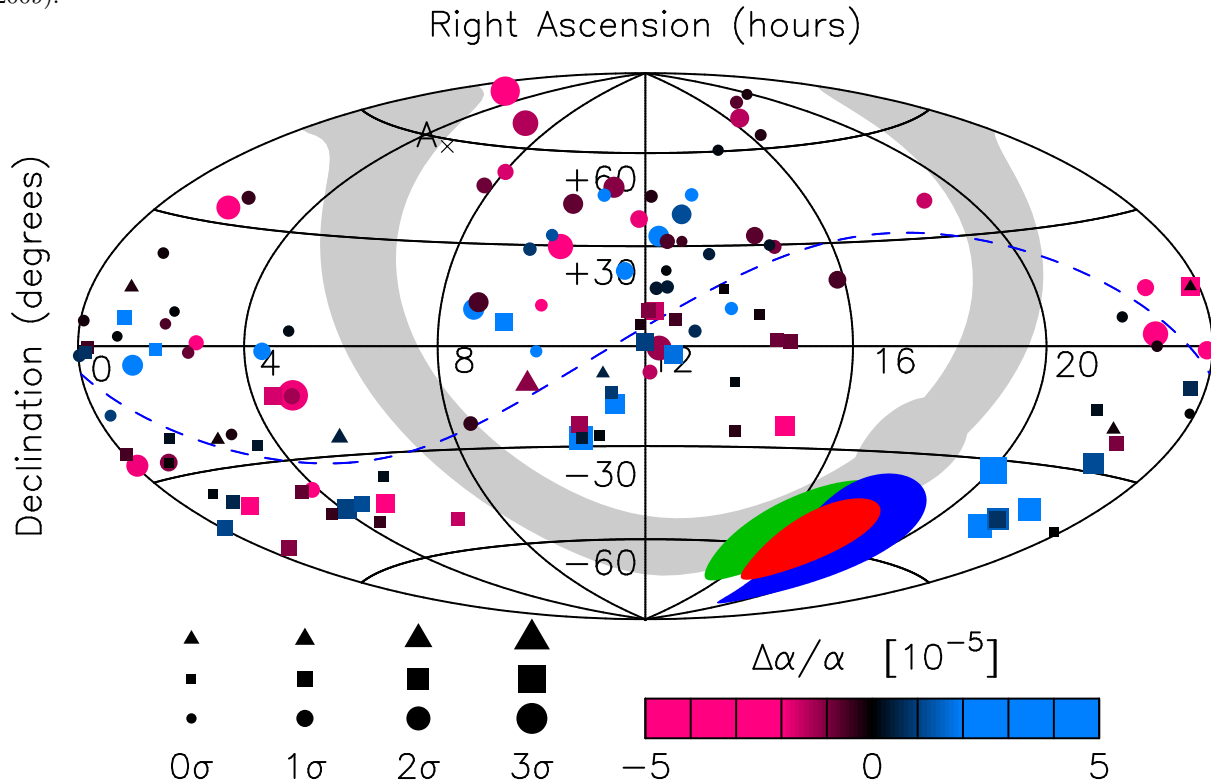


FIG. 5. Supplementary figure. Same all-sky illustration as in Fig. 1 showing the combined Keck and VLT $\Delta\alpha/\alpha$ measurements. Squares are VLT points. Circles are Keck points. Triangles are quasars observed at both Keck and VLT. Symbol size indicates deviation of $\Delta\alpha/\alpha$ from zero, i.e. $\Delta\alpha/\alpha = A \cos \Theta$. The blue dashed line shows the equatorial region. The grey shaded area shows the Galactic plane with the Galactic centre indicated as a bulge. More and larger blue squares are seen closer to the α -pole (red filled area) and more and larger red circles are seen closer to the α -antipole.